nature chemistry

ARTICLES

PUBLISHED ONLINE: 15 JANUARY 2012 | DOI: 10.1038/NCHEM.1242

Controlling on-surface polymerization by hierarchical and substrate-directed growth

L. Lafferentz[1,3], V. Eberhardt[2], C. Dri[3], C. Africh[3], G. Comelli[3,4], F. Esch[3†], S. Hecht[2*] and L. Grill[1*]

A key challenge in the field of nanotechnology, in particular in the design of molecular machines, novel materials or molecular electronics, is the bottom-up construction of covalently bound molecular architectures in a well-defined arrangement. To date, only rather simple structures have been obtained because of the limitation of one-step connection processes. Indeed, for the formation of sophisticated structures, step-by-step connection of molecules is required. Here, we present a strategy for the covalent connection of molecules in a hierarchical manner by the selective and sequential activation of specific sites, thereby generating species with a programmed reactivity. This approach leads to improved network quality and enables the fabrication of heterogeneous architectures with high selectivity. Furthermore, substrate-directed growth and a preferred orientation of the molecular nanostructures are achieved on an anisotropic surface. The demonstrated control over reactivity and diffusion during covalent bond formation constitutes a promising route towards the creation of sophisticated multi-component molecular nanostructures.

Assembling functional molecules directly on surfaces is an important objective in molecular nanotechnology. Well-defined arrangements of molecules in such architectures are necessary for the construction of sophisticated molecular machines[1], novel materials with specific characteristics[2,3] or nanocircuits for molecular electronics[4,5], promising dramatic improvements in terms of operation speed and energy consumption[6]. The ability of molecules to selectively interact with other molecules plays a key role in nature and can be used for their bottom-up assembly on surfaces. This characteristic has been successfully used in the past to grow a variety of molecular nanostructures on surfaces and to control the architectures by means of the chemical structures of the building blocks[7]. Based on different types of interactions (such as van der Waals[8], dipolar[9], hydrogen bonding[10] and metal–ligand interactions[11]; their strength increasing approximately in this order), a range of supramolecular assemblies can be formed on surfaces. However, for future applications, covalent bonding between building blocks holds more promise in terms of robustness and intermolecular charge transport and in recent years has been realized by various chemical reactions[12–21]. Most studies have been performed on clean surfaces using well-defined ultrahigh-vacuum conditions, as in this study, but polymerization in a solution environment is also feasible[22,23].

A versatile approach for the synthesis of macromolecules on a surface by covalent linking comprises the incorporation of specific, comparably weak intramolecular bonds in the monomer building blocks and the subsequent creation of reactive sites at these positions. This has been realized by the use of halogen–carbon bonds with lower bond energies than the organic framework at specific sites of the molecules[12] (inspired by the single-molecule synthesis of Hla and co-workers[24]). On heating, the halogen atoms are dissociated, creating reactive sites at their positions in a controlled fashion without breaking other molecular bonds (activation step). The activated molecular building blocks subsequently diffuse on the surface and connect with one another by forming covalent carbon–carbon bonds at the previous halogen sites (connection step). In this way, porphyrin nanostructures[12] and long and chemically homogeneous conjugated polyfluorenes, acting as molecular wires, could be formed[25], the latter even in the presence of inorganic crystallites[26]. This on-surface synthesis approach by halogen dissociation has also been used to connect smaller benzene- or thiophene-based monomers[19,27–29] and to assemble anthracene units to narrow graphene ribbons[3].

Various other chemical reactions have been reported for perylene-based molecules[15] and for the formation of imines[13,30], imides[31,32] and azobenzenes[33] on metallic surfaces. Moreover, it has been shown recently that polymerization reactions can also take place on ultrathin insulating films grown on a metal surface[34]. Considering the different linking chemistries developed so far, the direct connection of aromatic moieties is advantageous to establish π-conjugation for efficient charge transfer. In this context, the use of halogen substituents as activating groups[12] is highly promising, because the specific bond dissociation energy and thus activation temperature should be adjustable via the type of halogen atom, representing the conceptual starting point of this study.

So far, no hierarchical covalent linking reactions on surfaces have been achieved, which restricts the final structure to rather simple architectures. For the formation of sophisticated molecular nanostructures, instead, one has to choose a particular reaction pathway from the individual monomers to a pre-defined final architecture (Supplementary Fig. S3). This can be efficiently realized by partitioning the pathway into individual connection steps and controlling their sequence, thus guiding the assembly by kinetic control. The only way to achieve sequential growth is the stepwise provision of distinct reactive sites. Different dormant reactive sites that can be activated in a well-defined order must therefore be incorporated in the initial molecular building blocks. Here, we show for the first time how such a hierarchical growth can be realized by sequential activation of reactive sites and that additional control over

[1]Department of Physical Chemistry, Fritz-Haber-Institute of the Max-Planck-Society, 14195 Berlin, Germany, [2]Department of Chemistry, Humboldt-Universität zu Berlin, 12489 Berlin, Germany, [3]IOM-CNR Laboratorio TASC, Area Science Park, 34149 Basovizza-Trieste, Italy, [4]Physics Department and CENMAT, University of Trieste, 34127 Trieste, Italy; [†]Present address: Chemistry Department, Technische Universität München, 85748 Garching, Germany. *e-mail: lgr@fhi-berlin.mpg.de; sh@chemie.hu-berlin.de

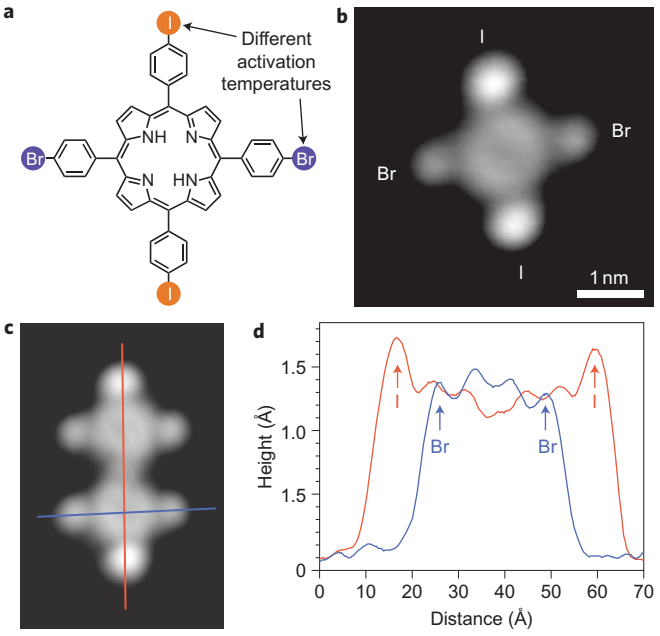

Figure 1 | Molecular building blocks with bromine and iodine substituents for sequential activation. a, Chemical structure of the ***trans*-Br_2I_2TPP** molecules. Bromine (blue) and iodine (red) leaving groups have different activation temperatures. **b**, STM image (bias voltage = 0.5 V, I = 0.1 nA) of a single ***trans*-Br_2I_2TPP** molecule on Au(111). Because of their chemical nature, the iodine substituents appear higher than the bromine substituents. **c**, STM image (4.3 × 6.5 nm^2) of a molecular dimer on Au(111). **d**, Height profiles taken along the lines in **c**.

hierarchical growth can be achieved using an anisotropic template surface. This approach leads to molecular nanostructures with greater sizes and allows the controlled formation of heterogeneous architectures. Our approach holds significant promise for the design of complex architectures and molecular circuits, a key issue in electronics composed of individual molecular entities.

Results and discussion

Molecular building blocks for hierarchical growth. To achieve hierarchical growth, we equipped a central molecular porphyrin building block with different halogen–phenyl side groups. These 5,15-bis(4′-bromophenyl)-10,20-bis(4′-iodophenyl)porphyrin (***trans*-Br_2I_2TPP**) molecules have two bromine and two iodine substituents, each in a linear *trans* configuration (Fig. 1a), to encode for the two directions of growth. The crucial point is that the bromine–phenyl and iodine–phenyl connections have different bond dissociation energies (for example, 336 kJ mol^{-1} for Br–C_6H_5 and 272 kJ mol^{-1} for I–C_6H_5 molecules in the gas phase[35]). The hierarchical concept is therefore encoded in the ***trans*-Br_2I_2TPP** molecule, because a combination of these two substituents should enable stepwise dissociation of the two halogen species, that is, initial thermal activation of the iodine sites and subsequent activation of the bromine sites at higher temperatures.

After deposition onto a Au(111) surface kept at room temperature, single molecules were imaged by low-temperature scanning tunnelling microscopy (STM) with submolecular resolution (Fig. 1b). The molecules appear as a central lobe with four legs, which correspond to the halogen–phenyl moieties. Because of their different chemical nature, the two halogen substituents appear at different characteristic heights and, in comparison with molecules with only one halogen species (see Supplementary Information), we can easily distinguish in the STM images the iodine and bromine substituents at the porphyrin building blocks. The brighter protrusions (apparent height of 1.7 ± 0.1 Å) represent the iodine substituents, with the bromine legs appearing lower (1.3 ± 0.1 Å), independent of bias voltage over the range used here (−1 V to +1 V).

Other than these intact species, after deposition onto the surface at room temperature, the major parts of the molecules are found as dimers and short chains that have lost at least one of their halogen substituents. An important characteristic of the oligomers (a dimer is shown in Fig. 1c) is that the individual monomers are always connected at previously iodine-terminated sites. This is evident from the height profiles (Fig. 1d), which show iodine substituents at the dimer terminals and bromine atoms sideways. Therefore, iodine atoms are dissociated from a part of the monomers upon adsorption, and the bromine–carbon bonds, because of their higher bond energy, remain intact at this stage, thus demonstrating the desired site selectivity for hierarchical growth. The covalent nature of the bonds is confirmed by the distance between the linked TPP units (17.6 ± 0.6 Å; 17.1 Å is obtained for a TPP dimer by density functional theory calculations[12]); a metal–ligand bond would give a significantly larger value[36]. This first 'snapshot' of molecular polymerization was further verified by lateral manipulation (revealing high stability) and voltage-dependent imaging, through which an unoccupied orbital, characteristic of the covalent bond, was visible at the bond position 3 eV above the Fermi level (see Supplementary Information).

Covalent connection by sequential activation. To achieve a fully controlled sequential activation sequence from the monomer via an intermediate reaction product to the final network (Fig. 2a), we deposited the ***trans*-Br_2I_2TPP** molecules onto a Au(111) sample kept at 80 K. Under these conditions, most of the molecules (98%) are found as intact monomers with all four halogen atoms attached (Fig. 2b), preferentially in close-packed arrangements. This observation indicates, in agreement with previous studies[37], a catalytic activity of the gold surface at room temperature, in contrast to the non-dissociative adsorption occurring at low temperatures.

After deposition at low temperatures (Fig. 2b), each adsorbed molecule contains both kinds of halogen substituents, and the thermal activation process can be initiated in a selective way. If the sample is heated to room temperature, partial iodine dissociation occurs, as in the deposition at room temperature described above. On further heating to 120 °C, efficient polymerization of the TPP molecules is induced via the selective activation of the terminal iodine substituents. Because of the *trans* configuration of the building blocks, linear chains of porphyrin molecules are created (Fig. 2c), which typically arrange in a parallel manner on the surface and form close-packed islands (Fig. 2e). At this stage, essentially no TPP monomers are found on the surface. In contrast to the chain formation from simple mono-functionalized *trans*-Br_2TPP molecules[12], the process occurs at a lower temperature and thus leaves the bromine groups intact, ready to be activated in the subsequent step.

In the next growth step, the remaining bromine substituents can be easily dissociated by supplying more thermal energy, that is, by heating to at least 200 °C (note that this is less than the temperature of ∼300 °C required for bromine dissociation in the evaporator[12], again indicating a catalytic activity of the gold surface[38]). Indeed, instead of linear chains (Fig. 2c), networks of molecules appear after heating the same sample to 250 °C (Fig. 2d). Thus, two-dimensional architectures are formed from the one-dimensional chains as soon as the bromine sites are activated and become available for interconnection of the chains. In contrast, when using the same procedure (as in Fig. 2) for **Br_4TPP** molecules, there is no sequential process—a one-step formation of networks is achieved instead, because only one type of halogen is available[12].

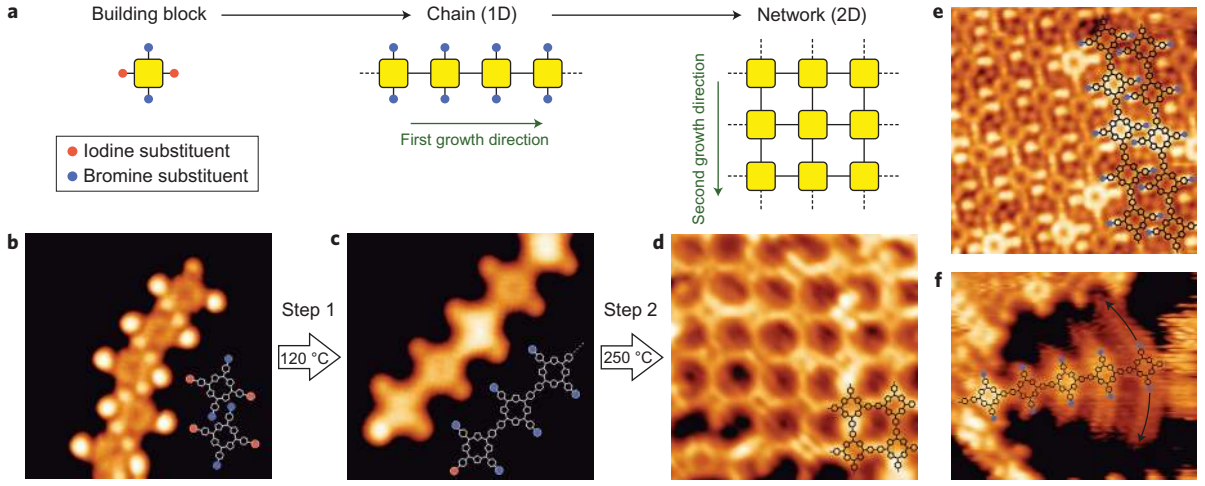

Figure 2 | Hierarchical growth following sequential thermal activation. a, Scheme of the sequential activation mechanism. Green arrows indicate the different growth directions of the two sequential steps. **b**–**d**, STM images (8 × 8 nm^2, **b**,**c**; 10 × 10 nm^2, **d**) of ***trans*-Br$_2$I$_2$TPP** molecules on Au(111): after deposition (at 80 K, **b**), after heating to 120 °C (**c**, Step 1), and after further heating to 250 °C (**d**, Step 2) (imaging at 180 °C). The corresponding chemical structures are indicated (for overview images, see Supplementary Information). The covalent nature of the created bonds is proven for all reaction steps. **e**, STM image (10 × 10 nm^2) of a close-packed polymer island after the first heating step. **f**, STM image (12 × 10 nm^2) of a TPP chain that is fixed at the left end and moving at the right end (indicated by arrows) due to the elevated sample temperature of 90 °C. This motion results in a 'Christmas tree' appearance, because molecular motion is faster than scanning (~10 s/image).

When conducting STM measurements at elevated temperatures, which are required for the polymerization process, the mobility and steric flexibility of single polymers can be directly imaged. Figure 2f depicts such a case, where a single chain, hooked at one end, continuously moves at the free end during imaging at a temperature of 90 °C, causing a 'Christmas tree' appearance of the moving chain. Probably in combination with this molecular flexibility, the equivalent structure of all molecular TPP chains leads to an important consequence in relation to two-dimensional growth: as soon as the first bond between two adjacent polymers chains is formed, they are automatically in a suitable arrangement for the formation of further bonds between them, because all activated sites are equally spaced along each chain. It is thus reasonable to expect that these covalently bound networks, sequentially linked in a hierarchical manner, exhibit less defects than those from a one-step growth procedure. Indeed, we find that the number of incorrectly connected molecular building blocks (for example, triangular instead of rectangular structures) is lower when using ***trans*-Br$_2$I$_2$TPP**, improving their regularity (see Supplementary Information). For instance, the number of triangular defects is significantly reduced by a factor of ~3. As a consequence of the reduced number of defects, the size of the regular networks is increased. Indeed, a detailed analysis for equivalent preparations also revealed larger networks for sequential activation (***trans*-Br$_2$I$_2$TPP** monomers; Fig. 3b) compared to one-step growth (**Br$_4$TPP** monomers; Fig. 3a). An interesting observation is that, as a result of the hierarchical mechanism, the nanostructures are found to be more elongated for ***trans*-Br$_2$I$_2$TPP** (in particular at small coverage) because polymers are linked in the second activation step, in comparison to the more uniform side lengths of networks achieved from **Br$_4$TPP** building blocks. Note that once connections have been formed, no self-repair of defects is possible, due to the irreversible nature of the covalent bonds.

Heterogeneous networks with high selectivity. The ability to sequentially activate specific groups within individual molecules paves the way towards the growth of heterogeneous molecular assemblies. Covalent assembly of different molecules on a metal surface under vacuum conditions has already been achieved by using two unequal species that can only couple to their complementary reaction partner, but in these one-step processes the final architecture is limited to a strict alternation of the two building blocks[13,17,30,32]. Alternatively, a random distribution of molecular assemblies would be formed in such a two-component system if all kinds of linking reactions were allowed in a one-step process. However, in both cases, there is no kinetic control over the process as the system always follows all reaction pathways. In the following, we show that it is possible to avoid a random distribution and indeed control the architecture, thus obtaining heterogeneous networks where the hierarchical process determines the final structure.

To achieve this goal, we used ***trans*-Br$_2$I$_2$TPP** in combination with dibromoterfluorene (**DBTF**) (Fig. 4a). The two species have an arrangement of iodine and bromine substituents that provide reactive sites at different activation temperatures. When depositing both types of molecules on the Au(111) surface and raising the sample temperature to 250 °C, the two reactions set in sequentially. First, the iodine substituents dissociate from the ***trans*-Br$_2$I$_2$TPP** molecules and the TPP molecules form chains. At this stage, the bromine substituents, because of their higher bond energy, are still intact and protect the potentially reactive sites in both types of molecules. Second, the bromine sites are activated and the **DBTF** molecules form chains that are attached to the porphyrin building blocks at the bromine sites (Fig. 4b). Although the chemical structures of **DBTF** and TPP are considerably different, coupling between the two species is not suppressed as in other cases[3], thus enabling the realization of the desired two-component architecture.

A detailed analysis of the covalent connections formed in these networks (Fig. 4c) reveals the very high selectivity of this process, with 98% of the former iodine sites at the porphyrin building blocks being used for connection to other porphyrin building blocks, and only 2% having fluorene molecules incorrectly attached. In contrast, at the bromine sites of the porphyrin building blocks, fluorene molecules are dominantly attached as a result of the second growth step. Binding of adjacent porphyrin chains to two-dimensional networks also occurs, giving rise to 30% of porphyrin molecules being attached at porphyrin bromine sites. The copolymers are thus formed with remarkable selectivity and the hierarchical concept seems very promising for the construction of more complex, heterogeneous architectures. Note that such kinetic control cannot be achieved without sequential activation,

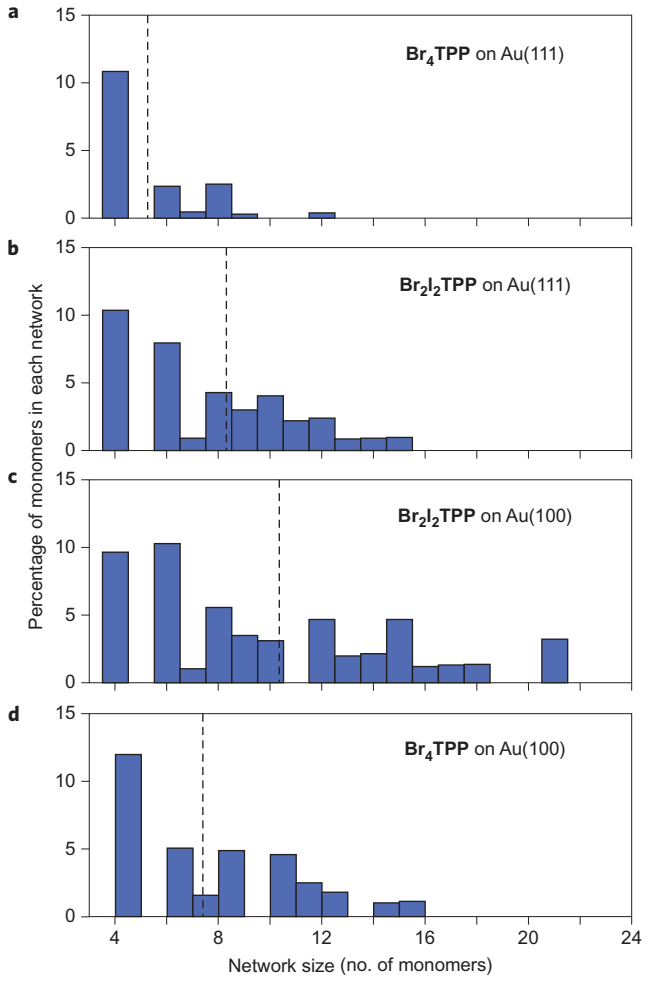

Figure 3 | Size distribution for non-hierarchical and hierarchical growth. Histograms of network size distribution for different preparations, showing that sequential activation leads to the formation of larger networks. The vertical dashed lines mark the average network size. Note that, as the objective is to grow two-dimensional networks, demanding rules for network counting have been applied, leading to smaller numbers for the dimensions of the covalently bound structures than would be obtained if all connections were considered (see Supplementary Information). The network size is given as the number of monomers involved in the networks, thus taking into account the molecular mass incorporated in each network. The total number of molecules, defining 100% and including also single molecules or assemblies that do not meet the counting rules, is ~1,200 for each case. Note that in all cases no counts exist for $n = 5$, because such pentamers are not possible according to the counting definitions.

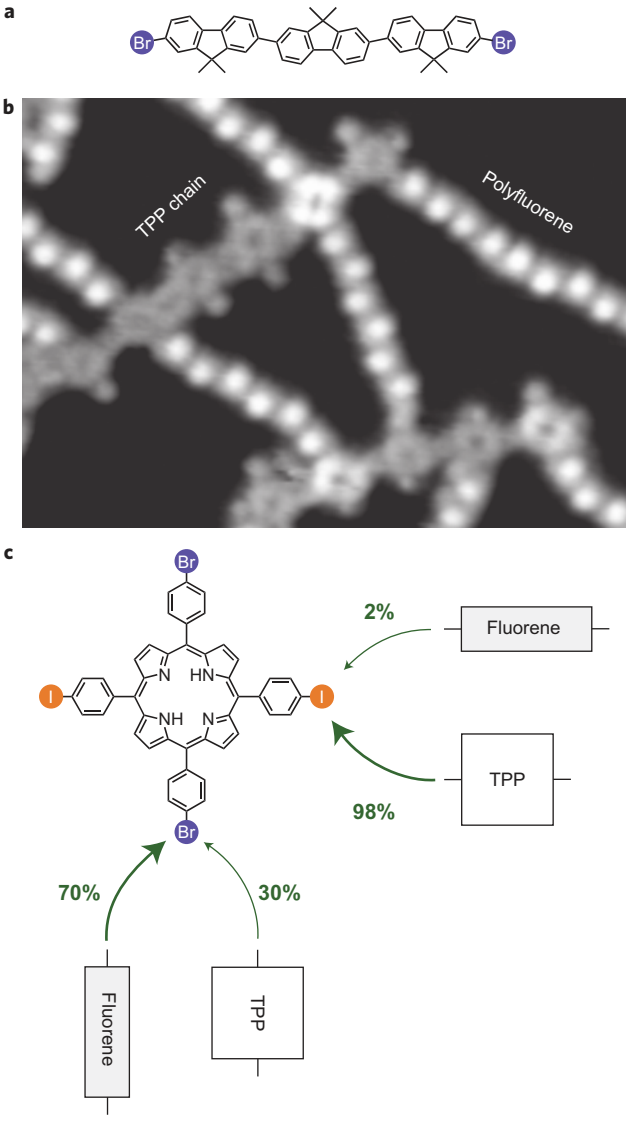

Figure 4 | Heterogeneous structures by hierarchical growth. a, Chemical structure of **DBTF**. **b**, STM image (13 × 18 nm^2) of a heterogeneous network grown from ***trans*-Br_2I_2TPP** and **DBTF** on Au(111) (after heating to 250 °C). **c**, Statistical analysis of porphyrin and fluorene attachment to the porphyrin (***trans*-Br_2I_2TPP**) building block at former iodine and bromine sites (total number of evaluated binding sites at the TPP molecules: $n_I = 489$, $n_{Br} = 269$).

as demonstrated by mixing **Br_4TPP** with **DBTF** molecules (Supplementary Fig. S7).

Substrate-directed hierarchical growth. The covalent linking of molecules by on-surface polymerization is based on two processes: activation and diffusion of the molecular building blocks on a surface. Note that elevated temperatures cause disorder of the molecular assemblies, which is unfavourable for efficient polymerization, and an additional means for improving molecular order is therefore desired. Having demonstrated the successful control of sequential activation with different chemical substituents, we now show how the polymerization can be further directed using a corrugated surface. It is of particular interest to obtain straight molecular chains with parallel orientation after the first hierarchical growth step, because this could lead to an improved connection to networks and potentially to a pre-defined network orientation on the surface. This could be achieved by using a corrugated surface, which can affect the process in two ways: (1) it can influence the molecular orientation, confining the created chains into specific orientations, and (2) it can direct molecular diffusion along the direction of the lowest corrugation. The latter effect has been observed on a Cu(110) surface[39], on which preferential alignment was also reported for a non-hierarchical one-step polymerization[27,29]. To test these effects of orientation and diffusion, we have chosen the Au(100) surface (see Supplementary Information), which reconstructs in a quasi-hexagonal (5 × 20) superstructure, featuring straight rows of vertically displaced atoms in the first layer[40]. This surface is structurally suitable for hosting polymer chains that cross the substrate rows with one molecule per row, because the corrugation is rather small (~0.7 Å) and the distance between rows (14.4 Å) is slightly below the intermolecular distance within the TPP polymers.

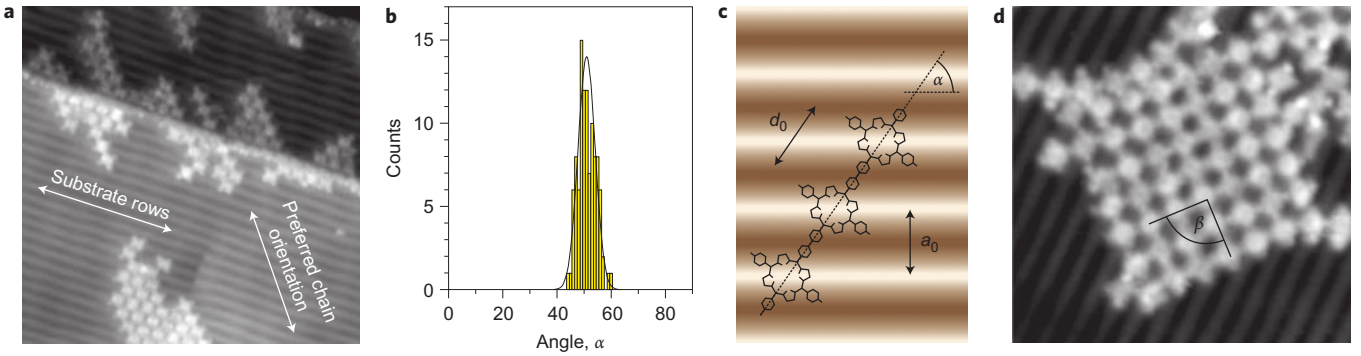

Figure 5 | Controlling covalent linking through substrate orientation. a, STM image (42 × 42 nm^2) of *trans*-Br_2TPP chains on Au(100) after the first growth step. **b**, Angular distribution for chains in **a**. **c**, Adsorption geometric scheme of the polymer on the Au(100) surface with $\alpha = 55^\circ$ for equivalent adsorption of all porphyrins ($a_o = 1.44$ nm and $d_o = 1.76$ nm). **d**, STM image (20 × 20 nm^2) of a single molecular network after the second activation step.

When depositing ***trans*-Br_2I_2TPP** onto the Au(100) surface, the monomers adsorb preferentially on top of the rows. After inducing the first activation step (by heating to 120 °C), we observe straight molecular chains with a preferential orientation (Fig. 5a). A detailed analysis of the angular distribution gives a preferred angle of ~51° between the chains and the atomic rows of the surface (Fig. 5b). This value is compatible with $\alpha = 55^\circ$, which is obtained if adjacent molecular building blocks are assumed to adsorb on neighbouring atomic rows (Fig. 5c). Hence, the chains are arranged in a pre-defined orientation that allows equivalent adsorption of all involved building blocks. Note that on Au(111), in contrast, the angular distribution of individual chains is less defined (see fig. 2h in ref. 12).

In analogy to the Au(111) case, network formation is also obtained on Au(100) upon heating at 250 °C (Fig. 5d). The preferential angle of the linear polymers after the first step ($\alpha = 51^\circ$) suggests that the two-dimensional structures, formed in the second step, might not be rectangular as on Au(111) (Fig. 2d). However, this is still the case for large networks because their configuration is determined by the large total intramolecular bond energy. On the other hand, the interaction with the surface dominates for very small assemblies, because the relative importance of the intramolecular bond energies is reduced (for example, one bond/molecule in a 2 × 2 network compared to 1.6 in a 5 × 5 network). Accordingly, the intramolecular bond angles (β in Fig. 5d) are rectangular for larger networks but $101 \pm 3^\circ$ for small structures comprising few connected monomers (see Supplementary Information). Moreover, the size of the networks is found to be higher than for the Au(111) case (Fig. 3b,c). We assign this to the directing role of the anisotropic Au(100) surface that leads to a preferentially parallel orientation of the TPP chains—presumably even during polymerization—and thus a more efficient covalent linking. Most notably, the networks exhibit a well-defined orientation with respect to the substrate, ~45° off the Au(100) atomic rows (Supplementary Fig. S10). Note that the use of **Br_4TPP** yields much smaller molecular structures on Au(100), confirming the importance of sequential activation. Hence, this approach of substrate-directed growth seems to fulfil both requirements for efficient polymerization—diffusion and pre-arrangement—simultaneously.

The influence of the Au(100) surface is also apparent when different molecules (***trans*-Br_2I_2TPP** and **DBTF**) are mixed. Directly after deposition, a mixed arrangement of the two species is observed (Fig. 6a), but higher order is created after the heating step, during which TPP networks and fluorene polymers form separate domains (Fig. 6b). This is in contrast to what is obtained on Au(111), in which **DBTF** and ***trans*-Br_2I_2TPP** molecules form separated islands before the heating process, which then leads to intermixing (Fig. 4). This result illustrates that the diffusion of intermediate products during hierarchical growth plays a key role. The observed segregation of the two polymer structures is probably caused by a confinement of the diffusion and reaction channels, thus illustrating an additional element of control.

With a view to further develop our hierarchical and directed growth approach, the option to use other non-thermal activation processes, such as photochemically induced dissociation, as well as exploring corrugated surfaces to selectively control the diffusion of various molecular components, is of particular interest. Specifically, substrate-directed growth in combination with top-down-engineered contacts appears an attractive route for connecting molecular nanostructures with the outside world. The central goal is the formation of sophisticated, structured arrays that incorporate specific functionalities at pre-defined positions. In this sense, this work represents a decisive step towards the controlled bottom-up construction of molecular machines and nanocircuits from single molecular components.

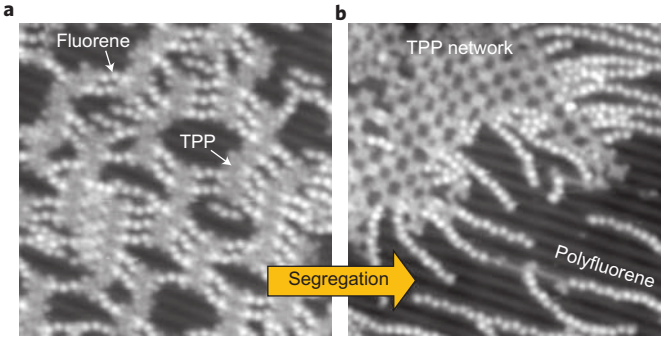

Figure 6 | Copolymerization and segregation on a Au(100) surface. a,**b**, STM images (32 × 32 nm^2) of a heterogeneous mixture of ***trans*-Br_2I_2TPP** and **DBTF** on Au(100) before (**a**) and after (**b**) heating to 250 °C.

Methods

The synthesis of ***trans*-Br_2I_2TPP** is described in the Supplementary Information, and the syntheses of **Br_4TPP** and **DBTF** have been reported previously[12,25]. STM images were taken at temperatures of 5–10 K (unless specified otherwise) with a modified Createc and an Omicron instrument and calibrated with atomically resolved images of the metal surface. STM experiments at room temperature and above were carried out with a modified Omicron variable-temperature STM (VT-STM). Imaging was performed in constant-current mode with a tunnelling current of 0.1 nA and tip–sample bias of 500 mV unless indicated otherwise. All experiments were carried out under ultrahigh-vacuum conditions with a base pressure of 1×10^{-10} mbar. In the low-temperature STM experiments, heating the sample to initiate polymerization was conducted on a manipulator followed by cooling and transfer into the STM, whereas the VT-STM allowed imaging at elevated temperatures.

The Au(111) and Au(100) samples were cleaned by conventional cycles of argon sputtering ($E = 1.5$ keV) and annealing to 530 °C. Molecules were evaporated from

a Knudsen cell at temperatures of ~200 °C (**DBTF** molecules) and 250 °C (porphyrin derivatives). The molecular flux was monitored using a quartz crystal microbalance.

Received 21 October 2011; accepted 30 November 2011; published online 15 January 2012

References

1. Browne, W. R. & Feringa, B. L. Making molecular machines work. *Nature Nanotech.* **1,** 25–35 (2006).
2. Whitesides, G. M., Mathias, J. P. & Seto, C. T. Molecular self-assembly and nanochemistry: a chemical strategy for the synthesis of nanostructures. *Science* **254,** 1312–1319 (1991).
3. Cai, J. *et al.* Atomically precise bottom-up fabrication of graphene nanoribbons. *Nature* **466,** 470–473 (2010).
4. Joachim, C., Gimzewski, J. K. & Aviram, A. Electronics using hybrid-molecular and mono-molecular devices. *Nature* **408,** 541–548 (2000).
5. Barth, J. V., Costantini, G. & Kern, K. Engineering atomic and molecular nanostructures at surfaces. *Nature* **437,** 671–679 (2005).
6. Heath, J. R. & Ratner, M. A. Molecular electronics. *Phys. Today* **56,** 43–49 (2003).
7. Bartels, L. Tailoring molecular layers at metal surfaces. *Nature Chem.* **2,** 87–95 (2010).
8. Rabe, J. P. & Buchholz, S. Commensurability and mobility in two-dimensional molecular patterns on graphite. *Science* **253,** 424–427 (1991).
9. Yokoyama, T., Yokoyama, S., Kamikado, T., Okuno, Y. & Mashiko, S. Selective assembly on a surface of supramolecular aggregates with controlled size and shape. *Nature* **413,** 619–621 (2001).
10. Slater, A. G., Beton, P. H. & Champness, N. R. Two-dimensional supramolecular chemistry on surfaces. *Chem. Sci.* **2,** 1440–1448 (2011).
11. Lin, N., Stepanow, S., Ruben, M. & Barth, J. V. Surface-confined supramolecular coordination chemistry. *Top. Curr. Chem.* **287,** 1–44 (2009).
12. Grill, L. *et al.* Nano-architectures by covalent assembly of molecular building blocks. *Nature Nanotech.* **2,** 687–691 (2007).
13. Weigelt, S. *et al.* Covalent interlinking of an aldehyde and an amine on an Au(111) surface in ultrahigh vacuum. *Angew. Chem. Int. Ed.* **46,** 9227–9230 (2007).
14. Champness, N. R. Surface chemistry: building with molecules. *Nature Nanotech.* **2,** 671–672 (2007).
15. Matena, M., Riehm, T., Stöhr, M., Jung, T. A. & Gade, L. H. Transforming surface coordination polymers into covalent surface polymers: linked polycondensed aromatics through oligomerization of *N*-heterocyclic carbene intermediates. *Angew. Chem. Int. Ed.* **47,** 2414–2417 (2008).
16. Veld, M. I., Iavicoli, P., Haq, S., Amabilino, D. B. & Raval, R. Unique intermolecular reaction of simple porphyrins at a metal surface gives covalent nanostructures. *Chem. Commun.* 1536–1538 (2008).
17. Zwaneveld, N. A. A. *et al.* Organized formation of 2D extended covalent organic frameworks at surfaces. *J. Am. Chem. Soc.* **130,** 6678–6679 (2008).
18. Gourdon, A. On-surface covalent coupling in ultrahigh vacuum. *Angew. Chem. Int. Ed.* **47,** 6950–6953 (2008).
19. Gutzler, R. *et al.* Surface mediated synthesis of 2D covalent organic frameworks: 1,3,5-tris(4-bromophenyl)benzene on graphite(001), Cu(111), and Ag(110). *Chem. Commun.* 4456–4458 (2009).
20. Perepichka, D. F. & Rosei, F. Extending polymer conjugation into the second dimension. *Science* **323,** 216–217 (2009).
21. Sakamoto, J., Heijst, J. v., Lukin, O. & Schlüter, A. D. Two-dimensional polymers: Just a dream of synthetic chemists? *Angew. Chem. Int. Ed.* **48,** 1030–1069 (2009).
22. Sakaguchi, H., Matsumura, H. & Gong, H. Electrochemical epitaxial polymerization of single-molecular wires. *Nature Mater.* **3,** 551–557 (2004).
23. Sakaguchi, H., Matsumura, H., Gong, H. & Abouelwafa, A. M. Direct visualization of the formation of single-molecule conjugated copolymers. *Science* **310,** 1002–1006 (2005).
24. Hla, S-W., Bartels, L., Meyer, G. & Rieder, K-H. Inducing all steps of a chemical reaction with the scanning tunneling microscope tip: towards single molecule engineering. *Phys. Rev. Lett.* **85,** 2777–2780 (2000).
25. Lafferentz, L. *et al.* Conductance of a single conjugated polymer as a continuous function of its length. *Science* **323,** 1193–1197 (2009).
26. Bombis, C. *et al.* Single molecular wires connecting metallic and insulating surface areas. *Angew. Chem. Int. Ed.* **48,** 9966–9970 (2009).
27. Lipton-Duffin, J. A., Ivasenko, O., Perepichka, D. F. & Rosei, F. Synthesis of polyphenylene molecular wires by surface-confined polymerization. *Small* **5,** 592–597 (2009).
28. Bieri, M. *et al.* Porous graphenes: two-dimensional polymer synthesis with atomic precision. *Chem. Commun.* 6919–6921 (2009).
29. Lipton-Duffin, J. A. *et al.* Step-by-step growth of epitaxially aligned polythiophene by surface-confined reaction. *Proc. Natl Acad. Sci.USA* **107,** 11200–11204 (2010).
30. Weigelt, S. *et al.* Surface synthesis of 2D branched polymer nanostructures. *Angew. Chem. Int. Ed.* **47,** 4406–4410 (2008).
31. Treier, M., Richardson, N. V. & Fasel, R. Fabrication of surface-supported low-dimensional polyimide networks. *J. Am. Chem. Soc.* **130,** 14054–14055 (2008).
32. Treier, M., Fasel, R., Champness, N. R., Argent, S. & Richardson, N. V. Molecular imaging of polyimide formation. *Phys. Chem. Chem. Phys.* **11,** 1209–1214 (2009).
33. Boz, S., Stöhr, M., Soydaner, U. & Mayor, M. Protecting-group-controlled surface chemistry—organization and heat-induced coupling of 4,4-di(tert-butoxycarbonylamino)biphenyl on metal surfaces. *Angew. Chem. Int. Ed.* **48,** 3179–3183 (2009).
34. Abel, M., Clair, S., Ourdjini, O., Mossoyan, M. & Porte, L. Single layer of polymeric Fe-phthalocyanine: an organometallic sheet on metal and thin insulating film. *J. Am. Chem. Soc.* **133,** 1203–1205 (2011).
35. Lide, D. R. (ed.) *CRC Handbook of Chemistry and Physics* 90th edn (CRC Press, 2010).
36. Villagomez, C. J., Sasaki, T., Tour, J. M. & Grill, L. Bottom-up assembly of molecular wagons on a surface. *J. Am. Chem. Soc.* **132,** 16848–16854 (2010).
37. Kanuru, V. K. *et al.* Sonogashira coupling on an extended gold surface *in vacuo*: Reaction of phenylacetylene with iodobenzene on Au(111). *J. Am. Chem. Soc.* **132,** 8081–8086 (2010).
38. Bieri, M. *et al.* Two-dimensional polymer formation on surfaces: insight into the roles of precursor mobility and reactivity. *J. Am. Chem. Soc.* **132,** 16669–16676 (2010).
39. Schunack, M. *et al.* Long jumps in the surface diffusion of large molecules. *Phys. Rev. Lett.* **88,** 156102 (2002).
40. Havu, P., Blum, V., Havu, V., Rinke, P. & Scheffler, M. Large-scale surface reconstruction energetics of Pt(100) and Au(100) by all-electron density functional theory. *Phys. Rev. B* **82,** 161418 (2010).

Acknowledgements

This work was funded by the Deutsche Forschungsgemeinschaft (DFG) through SFB 658 and European Projects ARTIST and AtMol. Funding from Fondo Trieste, MIUR (PRIN2008), CNR (NOMCIS) and the EU (NFFA) is gratefully acknowledged by the Trieste group.

Author contributions

S.H. and L.G. conceived the experiments. V.E. and S.H. synthesized the molecules. L.L., C.D., C.A., G.C., F.E. and L.G. performed the experiments. L.L., C.D. and L.G. analysed the data and L.G. wrote the paper. All authors discussed the results and commented on the manuscript.

Additional information

The authors declare no competing financial interests. Supplementary information and chemical compound information accompany this paper at www.nature.com/naturechemistry. Reprints and permission information is available online at http://www.nature.com/reprints. Correspondence and requests for materials should be addressed to S.H. and L.G.